GEOPHYSICS, VOL. 72, NO. 1 (JANUARY-FEBRUARY 2007); P. D9–D19, 7 FIGS.
10.1190/1.2387137

Plane-wave attenuation anisotropy in orthorhombic media

Yaping Zhu[1] and Ilya Tsvankin[2]

ABSTRACT

Orthorhombic models are often used in the interpretation of azimuthally varying seismic signatures recorded over fractured reservoirs. Here, we develop an analytic framework for describing the attenuation coefficients in orthorhombic media with orthorhombic attenuation (i.e., the symmetry of both the real and imaginary parts of the stiffness tensor is identical) under the assumption of homogeneous wave propagation. The analogous form of the Christoffel equation in the symmetry planes of orthorhombic and VTI (transversely isotropic with a vertical symmetry axis) media helps to obtain the symmetry-plane attenuation coefficients by adapting the existing VTI equations. To take full advantage of this equivalence with transverse isotropy, we introduce a parameter set similar to the VTI attenuation-anisotropy parameters ϵ_Q, δ_Q, and γ_Q. This notation, based on the same principle as Tsvankin's velocity-anisotropy parameters for orthorhombic media, leads to concise linearized equations for the symmetry-plane attenuation coefficients of all three modes (P, S_1, and S_2).The attenuation-anisotropy parameters also allow us to simplify the P-wave attenuation coefficient $\mathcal{A}_P$ outside the symmetry planes under the assumptions of small attenuation and weak velocity and attenuation anisotropy. The approximate coefficient $\mathcal{A}_P$ has the same form as the linearized P-wave phase-velocity function, with the velocity parameters $\epsilon^{(1,2)}$ and $\delta^{(1,2,3)}$ replaced by the attenuation parameters $\epsilon_Q^{(1,2)}$ and $\delta_Q^{(1,2,3)}$. The exact attenuation coefficient, however, also depends on the velocity-anisotropy parameters, while the body-wave velocities are almost unperturbed by the presence of attenuation. The reduction in the number of parameters responsible for the P-wave attenuation and the simple approximation for the coefficient $\mathcal{A}_P$ provide a basis for inverting P-wave attenuation measurements from orthorhombic media. The attenuation processing must be preceded by anisotropic velocity analysis that can be performed (in the absence of pronounced velocity dispersion) using existing algorithms for nonattenuative media.

INTRODUCTION

Effective velocity models of fractured reservoirs often have orthorhombic or an even lower symmetry (Schoenberg and Helbig, 1997; Bakulin et al., 2000). It is likely that polar and azimuthal velocity variations in orthorhombic formations are accompanied by directionally dependent attenuation. Indeed, systems of aligned fractures or pores are among the most common physical reasons for anisotropic attenuation (Mavko and Nur, 1979; Akbar et al., 1993; Parra, 1997; Stanchits et al., 2003; Maultzsch et al., 2003; Brajanovski et al., 2005). For example, Lynn et al. (1999) discuss the relationship between the azimuthal variation of attenuation and horizontal permeability measured over a fractured reservoir. MacBeth (1999) reviews some intrinsic attenuation mechanisms such as intracrack fluid flow and attributes the azimuthal variation of P-wave reflection amplitudes to attenuation anisotropy. Pointer et al. (2000) describe three different models of wave-induced fluid flow in cracked porous media; these models yield anisotropic velocities and attenuation coefficients when the cracks are aligned.

Other possible causes of attenuation anisotropy may include interbedding of thin attenuative layers (e.g., Carcione, 1992; Molotkov and Bakulin, 1998), stress-induced phenomena (e.g., Liu et al., 1993; Souriau and Romanowicz, 1996; Stanley and Christensen, 2001; Prasad and Nur, 2003), anisotropy of the density tensor in poroelastic Biot media (Bakulin and Molotkov, 1998), and azimuthal scattering (Willis et al., 2004).

Physical modeling shows that the P-wave attenuation coefficient in the direction perpendicular to aligned fractures or pores is higher than that parallel to the fractures (Akbar et al., 1993; Maultzsch et

Manuscript received by the Editor September 26, 2005; revised manuscript received September 15, 2006; published online December 29, 2006.
[1]Formerly Colorado School of Mines, Center for Wave Phenomena, Department of Geophysics, Golden, Colorado; presently ExxonMobil Upstream Research Company, P. O. Box 2189, Houston, Texas 77252. E-mail: yaping.zhu@exxonmobil.com.
[2]Colorado School of Mines, Center for Wave Phenomena, Department of Geophysics, Golden, Colorado 80401. E-mail: ilya@mines.edu.

al., 2003). Similar results were obtained by Hosten et al. (1987) for an orthorhombic sample made of composite material. On the whole, existing experimental data indicate that both velocity and attenuation in fractured rocks are angle-dependent, with the type and magnitude of the anisotropy controlled by such factors as the shape, distribution, type of infill, and orientation of aligned fractures and pores. When the dominant wavelength is much larger than the characteristic size of heterogeneities, the scattering phenomena can be ignored, and the medium can be treated as effectively homogeneous.

This paper is devoted to the macroscopic behavior of attenuation anisotropy and does not address the physical mechanisms that cause directionally dependent attenuation. We study the attenuation of plane waves propagating in a homogeneous medium that has orthorhombic symmetry for both the velocity function and attenuation coefficient.

The two main assumptions used here to facilitate the analytic description of attenuation are as follows:

1) Wave propagation is "homogeneous," which means that the real and imaginary parts of the complex wave vector, $\widetilde{\mathbf{k}} = \mathbf{k} - i\mathbf{k}^I$, are parallel to each other. This assumption is generally valid for point-source radiation in weakly attenuative media, but may lead to errors in the presence of strong attenuation or in describing reflection/transmission at medium interfaces. A detailed analysis of inhomogeneous plane-wave propagation in an unbounded, attenuative, anisotropic medium can be found in Červený and Pšenčík (2005a, 2005b).
2) The symmetry of the imaginary part of the complex stiffness matrix, $\widetilde{c}_{ij} = c_{ij} + ic^I_{ij}$, coincides with that of the real part (for orthorhombic media, we assume that c_{ij} and c^I_{ij} have the same orientation of the symmetry planes). This assumption ensures that the quality-factor matrix, $Q_{ij} \equiv c_{ij}/c^I_{ij}$ (Carcione, 2001), has the same structure as the real part of the stiffness matrix, which governs the velocity anisotropy. Note that the physical-modeling results of Hosten et al. (1987) indicate that the symmetry of the attenuation coefficient in an orthorhombic sample closely follows that of the velocity function.

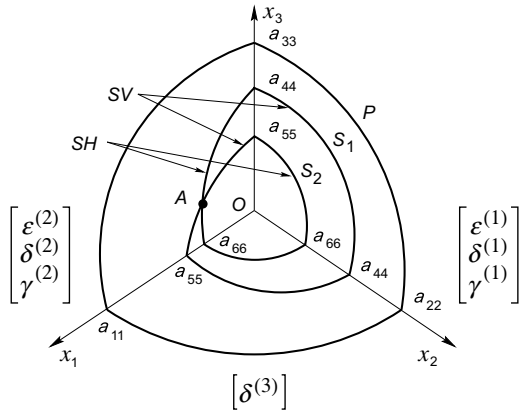

Figure 1. Sketch of the phase-velocity surfaces in orthorhombic media (after Tsvankin, 2005). $a_{ij} \equiv \sqrt{c_{ij}/\rho}$ are the normalized stiffness coefficients. Tsvankin's velocity-anisotropy parameters ($\epsilon^{(1,2)}$, $\delta^{(1,2,3)}$, and $\gamma^{(1,2)}$) are defined in the symmetry planes of the model, which coincide with the coordinate planes.

For homogeneous wave propagation, the wave vector is parallel to the unit vector $\mathbf{n}$ in the slowness direction: $\widetilde{\mathbf{k}} = \mathbf{n}(k - ik^I)$. Anisotropic attenuation can be characterized by the *normalized* attenuation coefficient $\mathcal{A}$ that determines the rate of amplitude decay per wavelength:

$$\mathcal{A} \equiv \frac{k^I}{k}. \tag{1}$$

The main challenge in describing the attenuation anisotropy in orthorhombic materials is in the large number of parameters that control the attenuation coefficients of P-, S_1-, and S_2-waves. Because of the coupling between the velocity and attenuation anisotropy, the coefficient $\mathcal{A}$ depends (for a fixed orientation of the symmetry planes) on the nine real stiffness coefficients and nine elements of the quality-factor matrix. Here, we show that significant progress can be achieved by extending the principle of Tsvankin's (1997) notation for velocity anisotropy (also, see Tsvankin, 2005) to attenuative orthorhombic media.

The equivalence between the complex Christoffel equations (Appendix A) in the symmetry planes of orthorhombic and VTI media makes it possible to obtain the symmetry-plane attenuation coefficients from the corresponding VTI equations. As discussed by Zhu and Tsvankin (2006), attenuation anisotropy in VTI media can be conveniently described by the Thomsen-style parameters ϵ_Q, δ_Q, and γ_Q. Using physical-modeling data, Zhu et al. (2007) demonstrate the feasibility of estimating these attenuation-anisotropy parameters from wide-angle amplitude measurements.

Adapting the results of Zhu and Tsvankin (2006) for the symmetry planes of orthorhombic media, we introduce seven anisotropy parameters responsible (in combination with the velocity parameters) for directionally dependent attenuation in orthorhombic materials. Linearizing the P-wave attenuation coefficient in the limit of small attenuation and weak anisotropy yields a simple expression outside the symmetry planes that has the same form as Tsvankin's (1997) approximate velocity function. The accuracy of this linearized solution is verified using numerical tests for models with substantial attenuation and velocity anisotropy.

To highlight the similarities between the anisotropy parameters for velocity and attenuation, we generally follow the organization of Tsvankin's (1997) paper in which he extended Thomsen's (1986) velocity-anisotropy notation to orthorhombic media. On the other hand, we emphasize distinct properties of attenuation anisotropy related to the coupling between the attenuation coefficient and velocity function.

EQUIVALENCE BETWEEN ATTENUATIVE ORTHORHOMBIC AND VTI MEDIA

We consider propagation of plane waves in orthorhombic media with orthorhombic attenuation under the assumption that the symmetry planes for the real and imaginary parts of the stiffness matrix have the same orientation (see above). It is convenient to choose a Cartesian coordinate system aligned with the natural coordinate frame of the model, so that each coordinate plane coincides with one of the three mutually orthogonal symmetry planes (Figure 1).

Plane-wave properties in anisotropic media are governed by the Christoffel equation, which has the same general form in attenuative and purely elastic models (Crampin, 1981; Helbig, 1994; Carcione, 2001). However, since in the presence of attenuation the polarization

and wave vectors become complex, the velocity function and attenuation coefficient are described by two coupled equations obtained by separating the real and imaginary parts of the Christoffel equation. For example, the Christoffel equation in the $[x_1,x_3]$ symmetry plane of attenuative orthorhombic media is given by

$$\begin{bmatrix} \tilde{c}_{11}\tilde{k}_1^2 + \tilde{c}_{55}\tilde{k}_3^2 - \rho\omega^2 & 0 & (\tilde{c}_{13} + \tilde{c}_{55})\tilde{k}_1\tilde{k}_3 \\ 0 & \tilde{c}_{66}\tilde{k}_1^2 + \tilde{c}_{44}\tilde{k}_3^2 - \rho\omega^2 & 0 \\ (\tilde{c}_{13} + \tilde{c}_{55})\tilde{k}_1\tilde{k}_3 & 0 & \tilde{c}_{55}\tilde{k}_1^2 + \tilde{c}_{33}\tilde{k}_3^2 - \rho\omega^2 \end{bmatrix} \begin{bmatrix} \tilde{U}_1 \\ \tilde{U}_2 \\ \tilde{U}_3 \end{bmatrix} = 0, \tag{2}$$

where ρ is the density, ω is the angular frequency, and $\tilde{\mathbf{U}}$ is the complex displacement (polarization) vector. Note that equation 2 is valid for any angle between the real and imaginary parts of the complex wave vector $\tilde{\mathbf{k}}$ and, therefore, is not limited to homogeneous wave propagation.

Equation 2 is almost identical to the Christoffel equation for VTI media with VTI attenuation, which is analyzed in detail by Zhu and Tsvankin (2006). The only difference between the two equations is that while for VTI media $\tilde{c}_{44} = \tilde{c}_{55}$, that is generally not the case for orthorhombic symmetry. However, the stiffness $\tilde{c}_{44}$ influences only the decoupled shear (SH) mode polarized perpendicular to the propagation plane $[x_1,x_3]$, while $\tilde{c}_{55}$ contributes to the velocity and attenuation of the in-plane polarized waves (P and SV). Therefore, the well-known equivalence between the Christoffel equation in purely elastic VTI media and symmetry planes of orthorhombic media (e.g., Tsvankin, 1997) holds for attenuative models, as long as the real and imaginary parts of the stiffness matrix have the same symmetry. In the regime of homogeneous wave propagation, the velocity and attenuation of all three modes in the $[x_1,x_3]$ plane are given by the results of Zhu and Tsvankin (2006) for VTI media.

The Christoffel equation in the symmetry planes $[x_2,x_3]$ and $[x_1,x_2]$ can be obtained from equation 2 by making the simple substitutions in the subscripts listed in Tsvankin (1997). Hence, the equivalence with vertical transverse isotropy is valid for the complex Christoffel equation in all three symmetry planes of attenuative orthorhombic media. This equivalence is used below to extend the VTI notation of Zhu and Tsvankin (2006) to orthorhombic models.

ATTENUATION-ANISOTROPY PARAMETERS

The Thomsen-style notation for velocity anisotropy introduced by Tsvankin (1997) facilitates the analytic description of a wide range of seismic signatures for orthorhombic models. Tsvankin's parameters provide a basis for inversion and processing of wide-azimuth data acquired over azimuthally anisotropic formations (Grechka and Tsvankin, 1999; Grechka et al., 1999, 2005; Bakulin et al., 2000). Here, we extend his approach to attenuative orthorhombic media with the main goal of defining the parameter combinations that govern the directionally dependent attenuation coefficient $\mathcal{A}$.

Since our notation is designed primarily for reflection data, we choose the P- and S-wave attenuation coefficients in the vertical (x_3) direction ($\mathcal{A}_{P0}$ and $\mathcal{A}_{S0}$) as the reference isotropic quantities. The coefficient $\mathcal{A}_{S0}$ corresponds to the S-wave polarized in the x_1-direction, which may be either the fast or slow shear mode, depending on the relationship between the stiffnesses c_{44} and c_{55}. The approximate (accurate to the second order in $1/Q$) coefficients $\mathcal{A}_{P0}$ and $\mathcal{A}_{S0}$ are given by

$$\mathcal{A}_{P0} \equiv \frac{1}{2Q_{33}}, \tag{3}$$

$$\mathcal{A}_{S0} \equiv \frac{1}{2Q_{55}}. \tag{4}$$

To characterize the attenuation of waves propagating in the $[x_1,x_3]$ plane, we define three attenuation-anisotropy parameters analogous to the Thomsen-style parameters ϵ_Q, δ_Q, and γ_Q introduced for VTI media with VTI attenuation by Zhu and Tsvankin (2006). The parameters $\epsilon_Q^{(2)}$ and $\gamma_Q^{(2)}$ (the superscript$^{(2)}$ stands for the x_2-axis perpendicular to the $[x_1,x_3]$ plane) determine the fractional difference between the attenuation coefficients in the x_1- and x_3-directions for P- and SH-waves, respectively. Another parameter, $\delta_Q^{(2)}$, is expressed through the second derivative of the P-wave attenuation coefficient $\mathcal{A}_P^{(2)}$ in the $[x_1,x_3]$ plane:

$$\epsilon_Q^{(2)} \equiv \frac{Q_{33} - Q_{11}}{Q_{11}}, \tag{5}$$

$$\delta_Q^{(2)} \equiv \frac{1}{2\mathcal{A}_{P0}} \left.\frac{d^2\mathcal{A}_P^{(2)}(\theta)}{d\theta^2}\right|_{\theta=0}$$

$$= \frac{\dfrac{Q_{33} - Q_{55}}{Q_{55}}\, c_{55}\dfrac{(c_{13} + c_{33})^2}{(c_{33} - c_{55})} + 2\dfrac{Q_{33} - Q_{13}}{Q_{13}}\, c_{13}\,(c_{13} + c_{55})}{c_{33}(c_{33} - c_{55})} \tag{6}$$

$$\approx 4\frac{Q_{33} - Q_{55}}{Q_{55}}g^{(2)} + 2\frac{Q_{33} - Q_{13}}{Q_{13}}(1 + 2\delta^{(2)} - 2g^{(2)}), \tag{7}$$

$$\gamma_Q^{(2)} \equiv \frac{Q_{44} - Q_{66}}{Q_{66}}, \tag{8}$$

where θ is the phase angle with the vertical, $g^{(2)} \equiv c_{55}/c_{33}$, and $\delta^{(2)}$ is a velocity-anisotropy parameter defined in the $[x_1,x_3]$ plane (Tsvankin, 1997). Equation 7 for $\delta_Q^{(2)}$ is simplified by dropping quadratic and higher-order terms in $g^{(2)}$ and $\delta^{(2)}$. Since the derivative of $\mathcal{A}_P^{(2)}$ is taken in the vertical direction, $\delta_Q^{(2)}$ governs the P-wave attenuation for near-vertical propagation in the $[x_1,x_3]$ plane.

Equations 5–8 are equivalent to the definitions of the corresponding VTI parameters. In contrast to VTI models, however, the stiffnesses and quality-factor elements of orthorhombic media with the subscripts 55 and 44 are generally different, and cannot be interchanged in equations 6–8.

Using the same substitutions in the subscripts ($11 \rightarrow 22$, $13 \rightarrow 23$, $55 \rightarrow 44$, and $44 \rightarrow 55$) as those in Tsvankin (1997), we introduce three attenuation-anisotropy parameters in the $[x_2,x_3]$ plane:

$$\epsilon_Q^{(1)} \equiv \frac{Q_{33} - Q_{22}}{Q_{22}}, \tag{9}$$

$$\delta_Q^{(1)} \equiv \frac{1}{2\mathcal{A}_{P0}} \left.\frac{d^2\mathcal{A}_P^{(1)}(\theta)}{d\theta^2}\right|_{\theta=0}$$

$$= \frac{\dfrac{Q_{33} - Q_{44}}{Q_{44}}\, c_{44}\dfrac{(c_{23} + c_{33})^2}{(c_{33} - c_{44})} + 2\dfrac{Q_{33} - Q_{23}}{Q_{23}}\, c_{23}\,(c_{23} + c_{44})}{c_{33}(c_{33} - c_{44})} \tag{10}$$

$$\approx 4\frac{Q_{33}-Q_{44}}{Q_{44}}g^{(1)} + 2\frac{Q_{33}-Q_{23}}{Q_{23}}(1+2\delta^{(1)}-2g^{(1)}), \tag{11}$$

$$\gamma_Q^{(1)} \equiv \frac{Q_{55}-Q_{66}}{Q_{66}}. \tag{12}$$

In equation 11, the attenuation coefficient $\mathcal{A}_P^{(1)}$ is measured in the $[x_2,x_3]$ plane as a function of the phase angle θ with the vertical, $g^{(1)} \equiv c_{44}/c_{33}$, and $\delta^{(1)}$ is a velocity-anisotropy parameter defined in the $[x_2,x_3]$ plane.

Since the attenuation coefficient is supposed to be positive (otherwise, the amplitude will increase with distance), the diagonal components of the Q_{ij} matrix must be positive as well. This constraint implies the parameters $\epsilon_Q^{(1)}$, $\epsilon_Q^{(2)}$, $\gamma_Q^{(1)}$, and $\gamma_Q^{(2)}$ are always larger than -1.

The only element of the Q_{ij} matrix not involved in the above definitions is Q_{12}. Following the approach of Tsvankin (1997), we use Q_{12} to introduce one more anisotropy parameter, $\delta_Q^{(3)}$, which plays the role of the VTI parameter δ_Q in the $[x_1,x_2]$ plane (x_1 is treated as the symmetry axis of the equivalent VTI model):

$$\delta_Q^{(3)} \equiv \frac{1}{2\mathcal{A}_P^{(3)}(\theta=0)} \left.\frac{d^2\mathcal{A}_P^{(3)}(\theta)}{d\theta^2}\right|_{\theta=0}$$
$$= \frac{\frac{Q_{11}-Q_{66}}{Q_{66}}c_{66}\frac{(c_{11}+c_{12})^2}{(c_{11}-c_{66})} + 2\frac{Q_{11}-Q_{12}}{Q_{12}}c_{12}(c_{12}+c_{66})}{c_{11}(c_{11}-c_{66})} \tag{13}$$

$$\approx 4\frac{Q_{11}-Q_{66}}{Q_{66}}g^{(3)} + 2\frac{Q_{11}-Q_{12}}{Q_{12}}(1+2\delta^{(3)}-2g^{(3)}), \tag{14}$$

where the coefficient $\mathcal{A}_P^{(3)}$ is measured in the $[x_1,x_2]$ plane as a function of the phase angle θ with the x_1 axis, $g^{(3)} \equiv c_{66}/c_{11}$, and $\delta^{(3)}$ is a velocity-anisotropy parameter defined in the $[x_1,x_2]$ plane. Although it is also possible to add the parameters $\epsilon_Q^{(3)}$ and $\gamma_Q^{(3)}$ in the $[x_1,x_2]$ plane, they would be redundant.

The nine attenuation-anisotropy parameters defined in equations 3–14, combined with Tsvankin's (1997) velocity-anisotropy parameters, are sufficient to fully characterize plane-wave attenuation in orthorhombic media. An additional practically important parameter responsible for the differential attenuation of the split S-waves in the vertical direction is introduced in the next section.

APPROXIMATE ATTENUATION COEFFICIENTS IN THE SYMMETRY PLANES

The equivalence with VTI media discussed above means that the symmetry-plane attenuation coefficients of all three modes can be obtained by adapting the corresponding VTI equations. While the exact attenuation coefficients are rather complicated even for VTI models and do not provide insight into the influence of various attenuation-anisotropy parameters, much simpler solutions can be found under the following assumptions used by Zhu and Tsvankin (2006):

1) The magnitude of attenuation measured by the inverse Q_{ij} values or the parameters $\mathcal{A}_{P0}$ and $\mathcal{A}_{S0}$ is small.
2) Attenuation anisotropy is weak, which implies that the absolute values of all attenuation-anisotropy parameters introduced above are much smaller than unity.
3) Velocity anisotropy is also weak, so the absolute values of all Tsvankin's (1997) anisotropy parameters are much smaller than unity.

The approximate (linearized in the small parameters) SH-wave attenuation coefficient in the $[x_1,x_3]$ plane can be written as

$$\mathcal{A}_{SH}^{(2)} = \bar{\mathcal{A}}_{S0}(1+\gamma_Q^{(2)}\sin^2\theta), \tag{15}$$

where θ is the phase angle with the vertical, and

$$\bar{\mathcal{A}}_{S0} = \frac{1}{2Q_{44}} = \mathcal{A}_{S0}\frac{1+\gamma_Q^{(1)}}{1+\gamma_Q^{(2)}} \tag{16}$$

is the vertical attenuation coefficient for the S-wave polarized in the x_2 direction. Equation 15 is obtained by replacing the parameter γ_Q in the linearized VTI result of Zhu and Tsvankin (2006) by $\gamma_Q^{(2)}$ and using the appropriate reference value $\bar{\mathcal{A}}_{S0}$. Similarly, the corresponding linearized coefficient in the $[x_2,x_3]$ plane has the form

$$\mathcal{A}_{SH}^{(1)} = \mathcal{A}_{S0}(1+\gamma_Q^{(1)}\sin^2\theta). \tag{17}$$

It should be emphasized that the term *SH-wave* refers to two different shear modes in the vertical symmetry planes (Tsvankin, 1997; see Figure 1). For example, if $c_{44} > c_{55}$, then the fast shear wave S_1 represents an SH-wave in the $[x_1,x_3]$ plane where it is polarized in the x_2 direction. For propagation in the $[x_2,x_3]$ plane, however, the S_1-wave becomes an SV mode that has an in-plane polarization vector.

The difference between the attenuation coefficients of the vertically traveling split shear waves can be quantified by the *attenuation splitting parameter* $\gamma_Q^{(S)}$:

$$\gamma_Q^{(S)} \equiv \left|\frac{\bar{\mathcal{A}}_{S0}-\mathcal{A}_{S0}}{\mathcal{A}_{S0}}\right| = \frac{|\gamma_Q^{(1)}-\gamma_Q^{(2)}|}{1+\gamma_Q^{(2)}} \approx |\gamma_Q^{(1)}-\gamma_Q^{(2)}|. \tag{18}$$

The definition in equation 18 is analogous to that of the widely used S-wave velocity-splitting parameter $\gamma^{(S)}$ (e.g., Helbig, 1994; Tsvankin, 2005). Although $\gamma_Q^{(S)}$ would be redundant as part of our notation for attenuative orthorhombic media, this parameter should play an important role in the attenuation analysis of shear-wave data.

Substituting the attenuation-anisotropy parameters $\epsilon_Q^{(2)}$ and $\delta_Q^{(2)}$ into the VTI equations of Zhu and Tsvankin (2006) yields the following approximate attenuation coefficients of the P- and SV-waves in the $[x_1,x_3]$ plane:

$$\mathcal{A}_P^{(2)} = \mathcal{A}_{P0}(1+\delta_Q^{(2)}\sin^2\theta\cos^2\theta + \epsilon_Q^{(2)}\sin^4\theta), \tag{19}$$

$$\mathcal{A}_{SV}^{(2)} = \mathcal{A}_{S0}(1+\sigma_Q^{(2)}\sin^2\theta\cos^2\theta), \tag{20}$$

where

$$\sigma_Q^{(2)} \equiv \frac{1}{g_Q^{(2)}}\left[2(1-g_Q^{(2)})\sigma^{(2)} + \frac{\epsilon_Q^{(2)}-\delta_Q^{(2)}}{g^{(2)}}\right], \tag{21}$$

$$g^{(2)} \equiv c_{55}/c_{33}, \quad g_Q^{(2)} \equiv Q_{33}/Q_{55} = \mathcal{A}_{S0}/\mathcal{A}_{P0},$$

and

$$\sigma^{(2)} \equiv (\epsilon^{(2)} - \delta^{(2)})/g^{(2)}.$$

The approximate attenuation coefficients in equations 19 and 20 have exactly the same form as the corresponding linearized phase-velocity equations (Tsvankin, 1997). However, the dependence of the attenuation-anisotropy parameter $\delta_Q^{(2)}$ (see equations 6 and 7) on the real parts of the stiffness coefficients reflects the coupling between the attenuation and velocity anisotropy. In contrast, the anisotropic phase-velocity function is practically independent of attenuation (see below). The linearized coefficients $\mathcal{A}_P^{(1)}$ and $\mathcal{A}_{SV}^{(1)}$ in the $[x_2,x_3]$ plane are adapted in the same way from the VTI equations by using the attenuation-anisotropy parameters $\epsilon_Q^{(1)}$ and $\delta_Q^{(1)}$.

AZIMUTHAL ANALYSIS OF P-WAVE ATTENUATION

Because of the difficulties in linearizing S-wave attenuation coefficients for out-of-plane phase directions, the scope of this section is limited to P-wave attenuation. While the attenuation of the split shear waves can be studied numerically by solving the Christoffel equation, the area of validity of such plane-wave solutions in describing radiation from seismic sources is significantly reduced by the distortions associated with S-wave point singularities (e.g., Crampin, 1991).

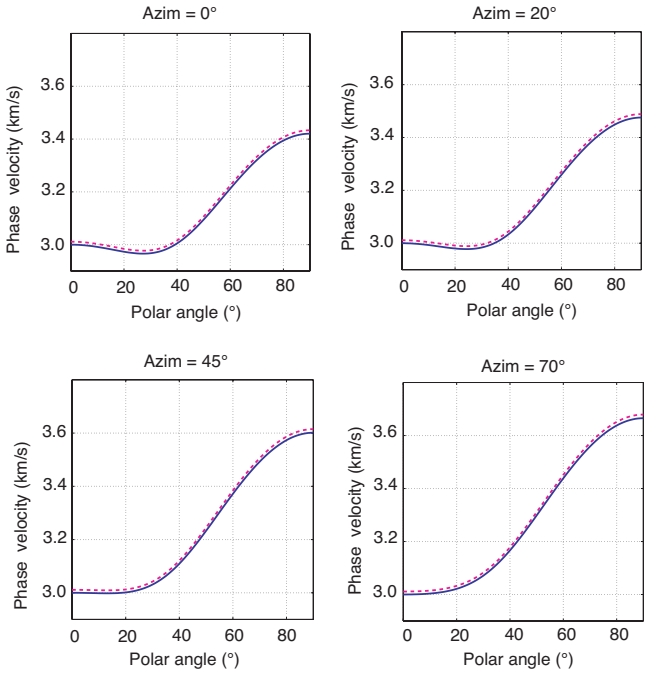

Figure 2. Influence of isotropic attenuation on the exact P-wave phase velocity in orthorhombic media computed from the Christoffel equation. Each plot corresponds to a fixed azimuthal phase angle. The solid curves mark the velocity for a nonattenuative orthorhombic model with the following parameters: $V_{P0} = 3$ km/s, $\epsilon^{(1)} = 0.25$, $\epsilon^{(2)} = 0.15$, $\delta^{(1)} = 0.05$, $\delta^{(2)} = -0.1$, and $\delta^{(3)} = 0.15$. The dashed curves are computed for a model with the same velocity parameters and strong isotropic attenuation [$Q_{33} = Q_{55} = 10$ ($\mathcal{A}_{P0} = \mathcal{A}_{S0} = 0.05$); all attenuation-anisotropy parameters are set to zero].

Influence of attenuation on phase velocity

As pointed out above, the attenuation coefficients depend not just on the quality-factor elements Q_{ij} but also on the velocity-anisotropy parameters. In contrast, the presence of attenuation has an almost negligible influence on the phase-velocity function in VTI media. This result remains valid for the symmetry planes of the orthorhombic model. Here, we demonstrate that attenuation-related distortions of phase velocity can be ignored outside the symmetry planes as well.

In the limit of weak attenuation ($1/Q_{ij} \ll 1$), the real part of the Christoffel equation A-1 can be simplified by dropping terms quadratic in the inverse Q components. The resulting equation A-3, which governs the velocity function, is identical to the Christoffel equation for the reference nonattenuative medium, both within and outside the symmetry planes.

To evaluate the contribution of the higher-order attenuation terms, we compute the exact P-wave phase velocity for two orthorhombic velocity models with strong attenuation. For the first model, the attenuation is isotropic with a very low quality factor, $Q_{33} = Q_{55} = 10$ (Figure 2). Still, the maximum attenuation-related change in the phase velocity is limited to 0.5%, which is equal to $1/2Q_{33}^2$.

The second model has the same real part of the stiffness matrix, but this time accompanied by pronounced attenuation anisotropy (Figure 3). Although the deviation of the phase-velocity function from that in the reference nonattenuative medium increases away from the vertical, it remains insignificant (up to 1%) for the whole range of polar and azimuthal phase angles. Although this analysis

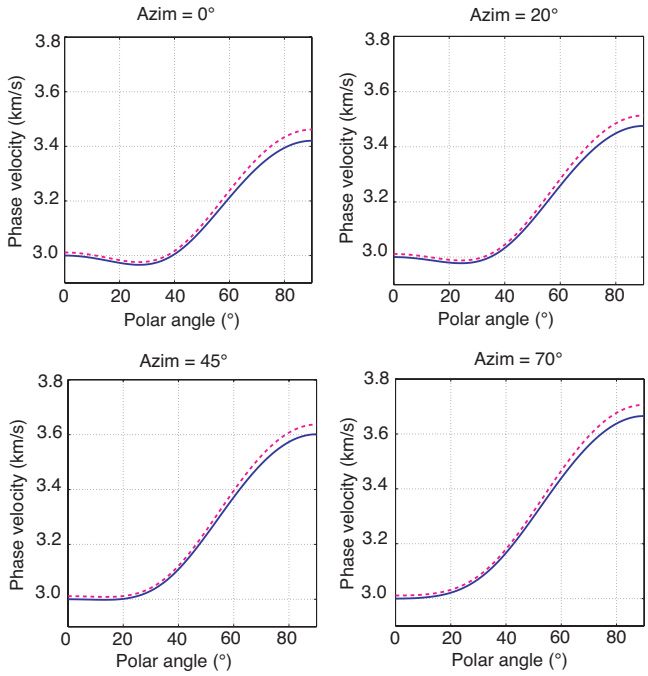

Figure 3. Influence of anisotropic attenuation on the exact P-wave phase velocity. The solid curves are the phase velocities for the nonattenuative orthorhombic model from Figure 2. The dashed curves are computed for a model with the same velocity parameters and strong orthorhombic attenuation: $Q_{33} = Q_{55} = 10$ ($\mathcal{A}_{P0} = \mathcal{A}_{S0} = 0.05$), $\epsilon_Q^{(1)} = \epsilon_Q^{(2)} = 0.8$, $\delta_Q^{(1)} = \delta_Q^{(2)} = \delta_Q^{(3)} = -0.5$, and $\gamma_Q^{(1)} = \gamma_Q^{(2)} = 0.8$.

does not take into account attenuation-related velocity dispersion, it is usually small in the frequency band typical for reflection seismology.

Hence, seismic processing for orthorhombic media with orthorhombic attenuation can be divided into two steps. First, one can perform anisotropic velocity analysis and estimation of Tsvankin's parameters without taking attenuation into account (e.g., Grechka and Tsvankin, 1999; Grechka et al., 2005). Then the reconstructed anisotropic-velocity model can be used in the processing of amplitude measurements and inversion for the attenuation-anisotropy parameters.

Approximate attenuation outside the symmetry planes

The linearized approximation for the P-wave attenuation coefficient is extended to arbitrary propagation directions outside the symmetry planes in the Appendix:

$$\mathcal{A}_P(\theta,\phi) = \mathcal{A}_{P0}[1 + \delta_Q(\phi)\sin^2\theta\cos^2\theta + \epsilon_Q(\phi)\sin^4\theta], \tag{22}$$

where θ is the phase angle with the vertical (i.e., the polar angle), ϕ is the phase angle with the x_1 axis (i.e., the azimuthal angle), and

$$\delta_Q(\phi) = \delta_Q^{(1)}\sin^2\phi + \delta_Q^{(2)}\cos^2\phi, \tag{23}$$

$$\epsilon_Q(\phi) = \epsilon_Q^{(1)}\sin^4\phi + \epsilon_Q^{(2)}\cos^4\phi + (2\epsilon_Q^{(2)} + \delta_Q^{(3)})\sin^2\phi\cos^2\phi. \tag{24}$$

Evidently, the approximate P-wave attenuation coefficient in any vertical plane ϕ = const is described by the VTI equation (Zhu and Tsvankin, 2006) with the azimuthally varying parameters $\epsilon_Q(\phi)$ and $\delta_Q(\phi)$. For wave propagation in the $[x_1,x_3]$ plane ($\phi = 0°$), $\epsilon_Q = \epsilon_Q^{(2)}$, $\delta_Q = \delta_Q^{(2)}$, and equation 22 reduces to equation 19. Similarly, for the $[x_2,x_3]$ plane ($\phi = 90°$), $\epsilon_Q = \epsilon_Q^{(1)}$ and $\delta_Q = \delta_Q^{(1)}$.

Interestingly, equations 22–24 have exactly the same form as the linearized P-wave phase-velocity equations (1.107–1.109) in Tsvankin (1997). This similarity is explained by the identical symmetry imposed on both the real and imaginary parts of the stiffness matrix and by the assumption of homogeneous wave propagation. However, an important difference between the coefficient $\mathcal{A}_P$ and the phase-velocity function is that the parameters $\delta_Q^{(1)}$, $\delta_Q^{(2)}$, and $\delta_Q^{(3)}$ include a contribution of the velocity anisotropy. In contrast, as shown above, phase velocity is practically independent of attenuation. Also, the exact coefficient $\mathcal{A}_P$ is influenced by the velocity-anisotropy parameters even for fixed values of $\delta_Q^{(1,2,3)}$; this is discussed in more detail below.

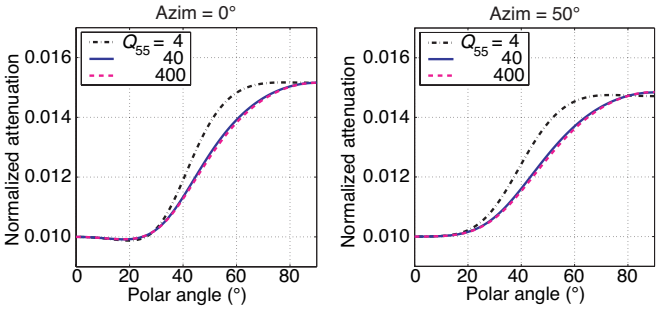

Figure 4. Influence of the parameter $\mathcal{A}_{S0}$ [$Q_{55} = 1/(2\mathcal{A}_{S0})$ is marked on the plot] on the exact P-wave attenuation coefficient. The relevant velocity-anisotropy parameters correspond to an orthorhombic model formed by vertical cracks embedded in a VTI background (Schoenberg and Helbig, 1997): $\epsilon^{(1)} = 0.329$, $\epsilon^{(2)} = 0.258$, $\delta^{(1)} = 0.083$, $\delta^{(2)} = -0.078$, and $\delta^{(3)} = -0.106$. The P-wave vertical attenuation coefficient is $\mathcal{A}_{P0} = 0.01$ ($Q_{33} = 50$); each relevant attenuation-anisotropy parameter is twice the corresponding velocity-anisotropy parameter: $\epsilon_Q^{(1)} = 0.658$, $\epsilon_Q^{(2)} = 0.516$, $\delta_Q^{(1)} = 0.166$, $\delta_Q^{(2)} = -0.156$, and $\delta_Q^{(3)} = -0.212$.

Transversely isotropic models with both vertical (VTI) and horizontal (HTI) symmetry axes represent special cases of orthorhombic media. For VTI media with VTI attenuation, all vertical planes are identical, and there is no velocity or attenuation variation in the horizontal (isotropy) plane:

$$\epsilon^{(1)} = \epsilon^{(2)} = \epsilon, \quad \epsilon_Q^{(1)} = \epsilon_Q^{(2)} = \epsilon_Q,$$

$$\delta^{(1)} = \delta^{(2)} = \delta, \quad \delta_Q^{(1)} = \delta_Q^{(2)} = \delta_Q,$$

$$\gamma^{(1)} = \gamma^{(2)} = \gamma, \quad \gamma_Q^{(1)} = \gamma_Q^{(2)} = \gamma_Q,$$

$$\delta^{(3)} = 0, \quad \delta_Q^{(3)} = 0.$$

Then $\epsilon_Q(\phi) = \epsilon_Q$, $\delta_Q(\phi) = \delta_Q$, and equation 22 reduces to the VTI result:

$$\mathcal{A}_P^{\mathrm{VTI}} = \mathcal{A}_{P0}(1 + \delta_Q\sin^2\theta\cos^2\theta + \epsilon_Q\sin^4\theta). \tag{25}$$

Next, suppose that the symmetry axis of the TI medium (for both velocity and attenuation) points in the x_1 direction. In this case, there are no property variations in the $[x_2,x_3]$ plane, and

$$\epsilon^{(1)} = \epsilon_Q^{(1)} = 0,$$

$$\delta^{(1)} = \delta_Q^{(1)} = 0,$$

$$\gamma^{(1)} = \gamma_Q^{(1)} = 0.$$

Also, the parameters $\delta^{(3)}$ and $\delta^{(2)}$ are no longer independent because the $[x_1,x_2]$ plane is equivalent to the $[x_1,x_3]$ plane. If the velocity anisotropy is weak, $\delta^{(3)} = \delta^{(2)} - 2\epsilon^{(2)}$ (Tsvankin, 1997). For weak attenuation anisotropy, $\delta_Q^{(3)} = \delta_Q^{(2)} - 2\epsilon_Q^{(2)}$, and equation 24 becomes $\epsilon_Q(\phi) = \epsilon_Q^{(2)}\cos^4\phi + \delta_Q^{(2)}\sin^2\phi\cos^2\phi$. Then the attenuation coefficient in equation 22 takes the form

$$\mathcal{A}_P^{\mathrm{HTI}} = \mathcal{A}_{P0}[1 + \delta_Q^{(2)}\cos^2\phi\sin^2\theta\cos^2\theta + (\epsilon_Q^{(2)}\cos^4\phi + \delta_Q^{(2)}\sin^2\phi\cos^2\phi)\sin^4\theta]. \tag{26}$$

Parameters for P-wave attenuation

The linearized P-wave attenuation coefficient in equation 22 is independent of the parameters $\mathcal{A}_{S0}$, $\gamma_Q^{(1)}$, and $\gamma_Q^{(2)}$, which are primarily responsible for S-wave attenuation. Numerical tests show that this conclusion remains valid for the exact coefficient $\mathcal{A}_P$ in models with strong attenuation and pronounced velocity and attenuation anisotropy. As illustrated by Figure 4, the dependence of $\mathcal{A}_P$ on the S-wave vertical attenuation coefficient $\mathcal{A}_{S0}$ becomes noticeable only for extremely large attenuation (i.e., uncommonly small values of Q_{55}). The influence of the parameters $\gamma_Q^{(1)}$ and $\gamma_Q^{(2)}$ on the coefficient $\mathcal{A}_P$ (not shown here) for typical moderately attenuative models is also negligible.

Therefore, for a fixed orientation of the symmetry planes and fixed velocity parameters, P-wave attenuation is controlled by the reference value $\mathcal{A}_{P0}$ and five attenuation-anisotropy parameters ($\epsilon_Q^{(1)}$, $\epsilon_Q^{(2)}$, $\delta_Q^{(1)}$, $\delta_Q^{(2)}$, and $\delta_Q^{(3)}$). An equivalent result for velocity anisotropy was obtained by Tsvankin (1997), who showed that the P-wave phase-velocity function in orthorhombic media is governed by just the vertical velocity V_{P0} and the parameters $\epsilon^{(1,2)}$ and $\delta^{(1,2,3)}$.

However, the numerical results discussed below reveal an important difference between attenuation and velocity anisotropy. Even if all attenuation-anisotropy parameters are held constant, the exact P-wave attenuation coefficient depends somewhat on the P-wave velocity-anisotropy parameters $\epsilon^{(1,2)}$ and $\delta^{(1,2,3)}$.[3]

Accuracy of the linearized solution and influence of the velocity parameters

To evaluate the accuracy of the weak-anisotropy approximation 22 outside the symmetry planes, we compare it with the exact coefficient $\mathcal{A}_P$ computed from the Christoffel equation for a model with pronounced orthorhombic attenuation (Figure 5). The velocity parameters correspond to the moderately anisotropic model of Schoenberg and Helbig (1997). Since no measurements of the attenuation-anisotropy parameters are available, each of them is set to be twice as large as the corresponding velocity-anisotropy parameter (e.g., $\epsilon_Q^{(2)} = 2\epsilon^{(2)}$).

As expected, the weak-anisotropy approximation gives satisfactory results for near-vertical propagation directions with polar angles up to about 30°. The error becomes more significant for intermediate propagation angles in the range $30° < \theta < 75°$. When the incidence plane is close to either vertical symmetry plane (i.e., the azimuth ϕ approaches 0° or 90°), the approximate solution also yields an accurate estimate of $\mathcal{A}_P$ near the horizontal direction. Overall, the error of the weak-anisotropy approximation for the full range of polar and azimuthal angles is less than 15%. Note that while the velocity anisotropy for this model is moderate (both $\epsilon^{(1)}$ and $\epsilon^{(2)}$ are about 0.3), the attenuation anisotropy is much more pronounced.

To identify the source of errors in the weak-anisotropy approximation, we repeat the test in Figure 5 using a purely isotropic velocity model (Figure 6). The approximate solution (dashed lines) in Fig-

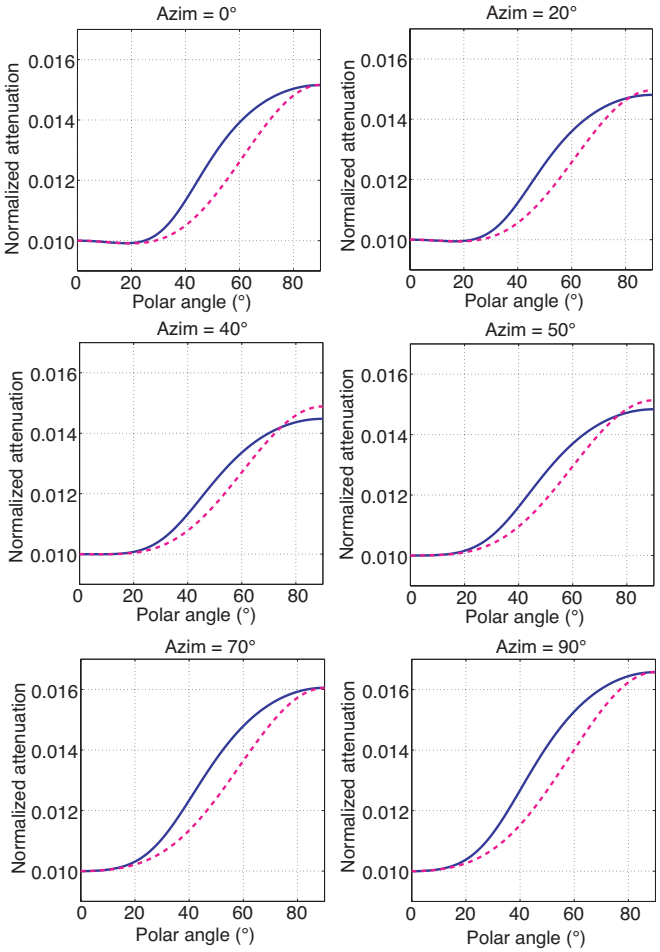

Figure 5. Comparison of the exact P-wave attenuation coefficient $\mathcal{A}_P$ (solid curves) with the linearized approximation 22 (dashed) for the model with orthorhombic velocity and attenuation from Figure 4 ($Q_{55} = 40$).

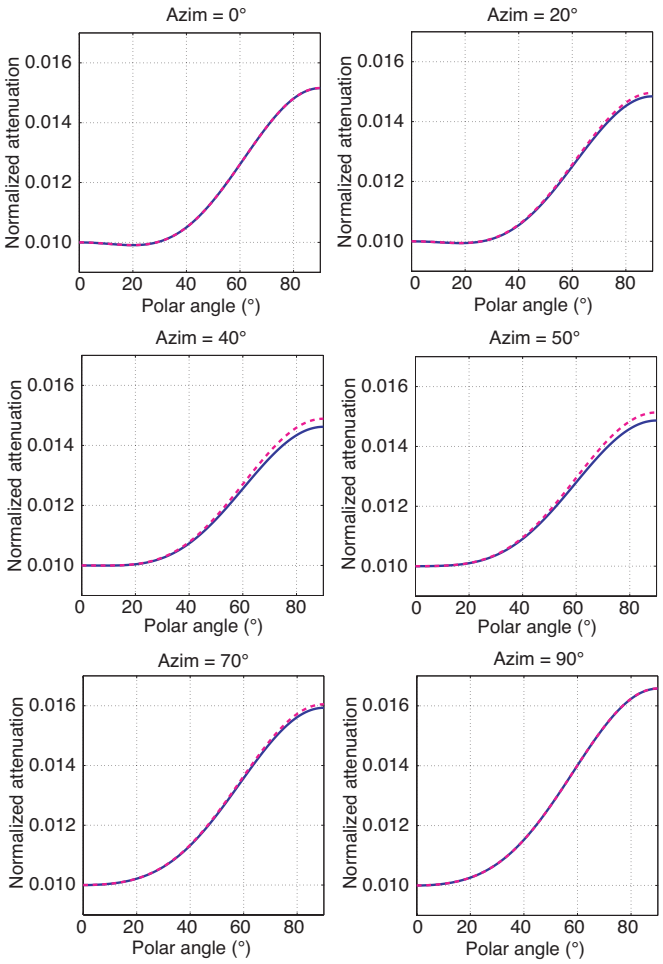

Figure 6. Comparison of the exact coefficient $\mathcal{A}_P$ (solid curves) with the linearized approximation 22 (dashed) for a medium with orthorhombic attenuation, but a purely isotropic velocity function. The attenuation parameters are the same as those in Figures 4 and 5, but all velocity-anisotropy parameters are set to zero.

[3]According to our numerical testing, P-wave attenuation is practically independent of the shear-wave velocity parameters $\gamma^{(1)}$ and $\gamma^{(2)}$.

ure 6 coincides with that in Figure 5, because the models have identical attenuation-anisotropy parameters. The exact attenuation coefficient $\mathcal{A}_P$ (solid lines), however, is influenced by the velocity-anisotropy parameters in such a way that the error of the weak-anisotropy approximation almost disappears when the velocity field is isotropic (Figure 6).

Hence, the accuracy of approximation 22 is controlled primarily by the strength of the P-wave *velocity* anisotropy. This can be explained by the multiple linearizations in the velocity-anisotropy parameters involved in deriving equations A-4 and A-7. Therefore, equation 22 gives an adequate qualitative description of P-wave attenuation (under the assumption of homogeneous wave propagation) for models with weak or moderate velocity anisotropy, even if the attenuation anisotropy is much stronger.

It should be emphasized that the contribution of different subsets of the velocity-anisotropy parameters to the attenuation coefficient $\mathcal{A}_P$ varies with the azimuth ϕ. As illustrated in Figure 7, the influence of the parameters $\epsilon^{(2)}$ and $\delta^{(2)}$ defined in the $[x_1,x_3]$ plane (i.e., for the azimuth $\phi = 0°$) decreases with azimuth and completely vanishes in the orthogonal (x_2) direction. Indeed, according to the Christoffel

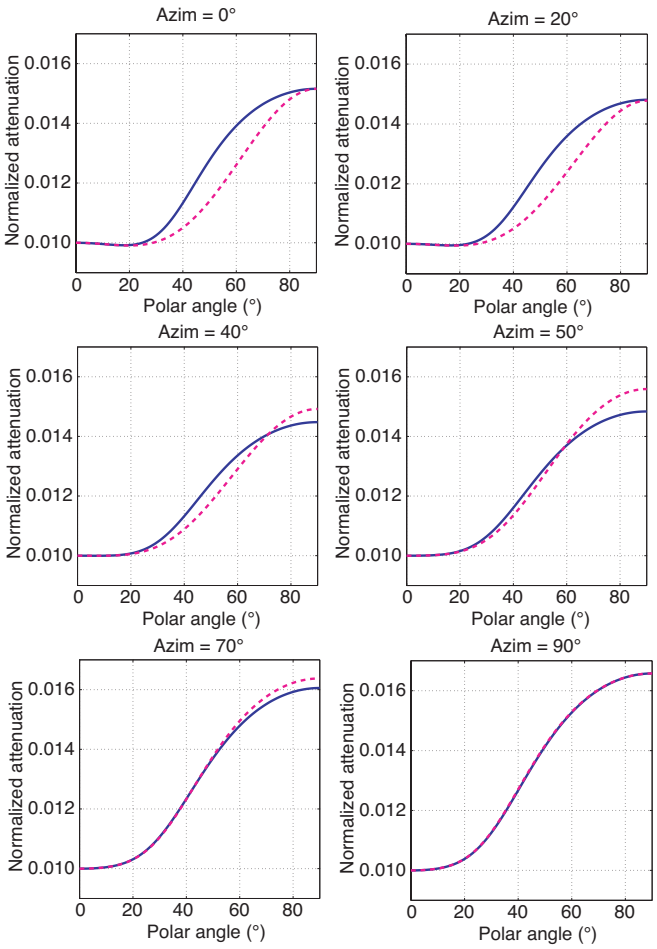

Figure 7. Influence of the P-wave velocity anisotropy on the exact attenuation coefficient $\mathcal{A}_P$. The solid curves are computed for the orthorhombic model with orthorhombic attenuation from Figures 4 and 5. The dashed curves are obtained by setting the velocity-anisotropy parameters $\epsilon^{(2)}$ and $\delta^{(2)}$ defined in the $[x_1,x_3]$ plane (azimuth $\phi = 0°$) to zero; all other model parameters are unchanged.

equation, the exact P-wave attenuation coefficient in either vertical-symmetry plane is fully determined by the velocity- and attenuation-anisotropy parameters defined in that plane.

CONCLUSIONS

The attenuation coefficients of P-, S_1-, and S_2-waves in orthorhombic media with orthorhombic attenuation depend on the orientation of the symmetry planes, nine velocity parameters, and nine components of the quality-factor matrix. The large number of independent parameters, compounded by the coupling between the attenuation and velocity anisotropy, makes attenuation analysis for this model extremely difficult. Here, we demonstrated that the description of attenuation coefficients in orthorhombic media can be substantially simplified by introducing a set of attenuation-anisotropy parameters similar to Tsvankin's notation for the velocity function. While we do not use any specific physical model, it is assumed that the real and imaginary parts of the stiffness tensor have identical symmetry and wave propagation is homogeneous (i.e., the inhomogeneity angle is negligible).

The equivalence between the Christoffel equation in the symmetry planes of orthorhombic and VTI media, established previously for purely elastic media, holds in the presence of orthorhombic attenuation. Therefore, the symmetry-plane attenuation coefficients of all three modes can be obtained by simply adapting the known VTI equations. Also, our Thomsen-style notation for attenuative VTI media can be extended to orthorhombic models following the approach suggested by Tsvankin for velocity anisotropy. The parameter set introduced here includes the vertical P- and S-wave attenuation coefficients ($\mathcal{A}_{P0}$ and $\mathcal{A}_{S0}$) and seven dimensionless anisotropy parameters ($\epsilon_Q^{(1,2)}$, $\delta_Q^{(1,2,3)}$, and $\gamma_Q^{(1,2)}$).

Adaptation of the approximate VTI equations allows us to obtain concise symmetry-plane attenuation coefficients of P-, S_1-, and S_2-waves valid for small attenuation and weak velocity and attenuation anisotropy. Furthermore, linearization of the Christoffel equation in the anisotropy parameters yields the P-wave attenuation coefficient $\mathcal{A}_P$ outside the symmetry planes as a simple function of $\mathcal{A}_{P0}$, $\epsilon_Q^{(1,2)}$, and $\delta_Q^{(1,2,3)}$. The influence of the parameters $\mathcal{A}_{S0}$ and $\gamma_Q^{(1,2)}$ on P-wave attenuation is negligible even for large attenuation anisotropy.

The linearized coefficient $\mathcal{A}_P$ has the same form as the approximate P-wave phase-velocity function in terms of Tsvankin's velocity parameters and can be represented by the VTI equation with the azimuthally varying parameters ϵ_Q and δ_Q. This equivalence between the linearized equations for attenuation and velocity anisotropy stems from the identical (orthorhombic) symmetry of the real and imaginary parts of the stiffness tensor and from the assumption of homogeneous wave propagation. Still, there are important differences between the treatment of velocity and attenuation anisotropy. In the absence of pronounced velocity dispersion, the influence of attenuation (i.e., of the imaginary part of the stiffness tensor) on velocity is practically negligible. In contrast, the definitions of the attenuation-anisotropy parameters $\delta_Q^{(1,2,3)}$ include the velocity parameters $\delta^{(1,2,3)}$.

Also, the exact attenuation coefficient $\mathcal{A}_P$ is somewhat dependent on the P-wave velocity-anisotropy parameters $\epsilon^{(1,2)}$ and $\delta^{(1,2,3)}$, even for fixed values of $\mathcal{A}_{P0}$, $\epsilon_Q^{(1,2)}$, and $\delta_Q^{(1,2,3)}$. Moreover, the accuracy of the linearized equation for $\mathcal{A}_P$ is controlled to a large degree by the strength of the P-wave velocity anisotropy. Numerical tests demonstrate that the approximate $\mathcal{A}_P$ remains close to the exact value even

for large (by absolute value) attenuation-anisotropy parameters, provided the velocity anisotropy is moderate.

Thus, the P-wave attenuation coefficient is governed primarily by the orientation of the symmetry planes and six (instead of nine) attenuation-anisotropy parameters: $\mathcal{A}_{P0}$, $\boldsymbol{\epsilon}_Q^{(1,2)}$, and $\boldsymbol{\delta}_Q^{(1,2,3)}$. However, since for models with pronounced velocity variations, $\mathcal{A}_P$ is also influenced by the parameters $\boldsymbol{\epsilon}^{(1,2)}$ and $\boldsymbol{\delta}^{(1,2,3)}$, accurate inversion of attenuation measurements may have to involve anisotropic velocity analysis. Also, knowledge of the anisotropic velocity field is needed to obtain the normalized attenuation coefficient $\mathcal{A}$ and to correct for the difference between the phase attenuation coefficient studied here and the group attenuation coefficient responsible for the amplitude decay along seismic rays. Overall, these results provide an analytic foundation for estimating the attenuation-anisotropy parameters from wide-azimuth seismic data.

Whereas this study is restricted to homogeneous wave propagation, the inhomogeneity angle in layered attenuative media is not necessarily small, and its influence deserves further analysis. We also assumed that the symmetry planes for the velocity and attenuation functions are aligned, which is justified for effective azimuthally anisotropic media caused by systems of parallel fractures. Still, for more complicated porous, fractured models, this assumption may break down, and most of our developments would need to be revised. Finally, if the quality-factor matrix varies with frequency, the attenuation-anisotropy parameters also become frequency-dependent, although their definitions remain the same.

ACKNOWLEDGMENTS

We are grateful to members of the A(nisotropy)-Team of the Center for Wave Phenomena (CWP), Colorado School of Mines (CSM), for helpful discussions. We would like to thank Ken Larner (CSM), Andrey Bakulin (Shell E&P), and the associate editor of GEOPHYSICS for their reviews of the manuscript. The support for this work was provided by the Consortium Project on Seismic Inverse Methods for Complex Structures at CWP.

APPENDIX A

APPROXIMATE ATTENUATION OUTSIDE THE SYMMETRY PLANES OF ORTHORHOMBIC MEDIA

The complex Christoffel equation for homogeneous wave propagation outside the symmetry planes can be written as

$$
\begin{aligned}
&[(c_{11}n_1^2 + c_{66}n_2^2 + c_{55}n_3^2)\mathcal{K}_{1,(1,6,5)} - \rho V^2 + i(c_{11}n_1^2 + c_{66}n_2^2 \\
&\quad + c_{55}n_3^2)\mathcal{K}_{2,(1,6,5)}] \times \{[(c_{66}n_1^2 + c_{22}n_2^2 + c_{44}n_3^2)\mathcal{K}_{1,(6,2,4)} \\
&\quad - \rho V^2 + i(c_{66}n_1^2 + c_{22}n_2^2 + c_{44}n_3^2)\mathcal{K}_{2,(6,2,4)}] \times [(c_{55}n_1^2 \\
&\quad + c_{44}n_2^2 + c_{33}n_3^2)\mathcal{K}_{1,(5,4,3)} - \rho V^2 + i(c_{55}n_1^2 + c_{44}n_2^2 \\
&\quad + c_{33}n_3^2)\mathcal{K}_{2,(5,4,3)}] - [(c_{23} + c_{44})n_2n_3(\mathcal{K}_{1,(23,44)} \\
&\quad + i\mathcal{K}_{2,(23,44)})]^2\} - [(c_{12} + c_{66})n_1n_2(\mathcal{K}_{1,(12,66)} \\
&\quad + i\mathcal{K}_{2,(12,66)})] \times \{[(c_{12} + c_{66})n_1n_2(\mathcal{K}_{1,(12,66)} \\
&\quad + i\mathcal{K}_{2,(12,66)})] \times [(c_{55}n_1^2 + c_{44}n_2^2 + c_{33}n_3^2)\mathcal{K}_{1,(5,4,3)} \\
&\quad - \rho V^2 + i(c_{55}n_1^2 + c_{44}n_2^2 + c_{33}n_3^2)\mathcal{K}_{2,(5,4,3)}] \\
&\quad - [(c_{13} + c_{55})n_1n_3(\mathcal{K}_{1,(13,55)} + i\mathcal{K}_{2,(13,55)})] \times [(c_{23} \\
&\quad + c_{44})n_2n_3(\mathcal{K}_{1,(23,44)} + i\mathcal{K}_{2,(23,44)})]\} \\
&\quad + [(c_{13} + c_{55})n_1n_3(\mathcal{K}_{1,(13,55)} + i\mathcal{K}_{2,(13,55)})] \times \{[(c_{12} \\
&\quad + c_{66})n_1n_2(\mathcal{K}_{1,(12,66)} + i\mathcal{K}_{2,(12,66)})] \times [(c_{23} + c_{44}) \\
&\quad \times n_2n_3(\mathcal{K}_{1,(23,44)} + i\mathcal{K}_{2,(23,44)})] - [(c_{13} + c_{55})n_1n_3 \\
&\quad \times (\mathcal{K}_{1,(13,55)} + i\mathcal{K}_{2,(13,55)})][(c_{66}n_1^2 + c_{22}n_2^2 + c_{44}n_3^2) \\
&\quad \times \mathcal{K}_{1,(6,2,4)} - \rho V^2 + i(c_{66}n_1^2 + c_{22}n_2^2 + c_{44}n_3^2) \\
&\quad \times \mathcal{K}_{2,(6,2,4)}]\} = 0, \qquad \text{(A-1)}
\end{aligned}
$$

where

$$\mathcal{K}_1 = 1 - \mathcal{A}^2 + \frac{2}{Q_{33}}\mathcal{A}, \quad \mathcal{K}_2 = \frac{1 - \mathcal{A}^2}{Q_{33}} - 2\mathcal{A},$$

$$\mathcal{K}_{1,(i,j,l)} = \mathcal{K}_1 + 2\frac{\Delta_{(i,j,l)}}{Q_{33}}\mathcal{A},\ \mathcal{K}_{2,(i,j,l)} = \mathcal{K}_2 + \frac{\Delta_{(i,j,l)}}{Q_{33}}(1 - \mathcal{A}^2),$$

$$\mathcal{K}_{1,(ij,kl)} = \mathcal{K}_1 + 2\frac{\Delta_{(ij,kl)}}{Q_{33}}\mathcal{A},\ \mathcal{K}_{2,(ij,kl)} = \mathcal{K}_2 + \frac{\Delta_{(ij,kl)}}{Q_{33}}(1 - \mathcal{A}^2),$$

$$\Delta_{(i,j,l)} = \frac{c_{ii}n_1^2\dfrac{Q_{33} - Q_{ii}}{Q_{ii}} + c_{jj}n_2^2\dfrac{Q_{33} - Q_{jj}}{Q_{jj}} + c_{ll}n_3^2\dfrac{Q_{33} - Q_{ll}}{Q_{ll}}}{c_{ii}n_1^2 + c_{jj}n_2^2 + c_{ll}n_3^2},$$

$$\Delta_{(ij,kl)} = \frac{c_{ij}\dfrac{Q_{33} - Q_{ij}}{Q_{ij}} + c_{kl}\dfrac{Q_{33} - Q_{kl}}{Q_{kl}}}{c_{ij} + c_{kl}}.$$

Note that $\mathcal{A} \equiv k'/k$ is on the order of the inverse Q-factor $(1/Q)$. When the attenuation is weak ($\mathcal{A} \ll 1$), we obtain $\mathcal{K}_1 \approx 1$ and $\mathcal{K}_2 \approx 1/Q_{33} - 2\mathcal{A}$ by dropping the quadratic and higher-order terms in $\mathcal{A}$ (i.e., in $1/Q$). Assuming that Q_{33} and Q_{55} are of the same order (the common case), weak-attenuation anisotropy implies the same order for all components Q_{ij}. Hence, the magnitude of the terms $\Delta_{(i,j,l)}$ and $\Delta_{(ij,kl)}$ cannot be much larger than unity. Then the terms $(\Delta_{(i,j,l)}/Q_{33})\mathcal{A}$, $(\Delta_{(ij,kl)}/Q_{33})\mathcal{A}$, $(\Delta_{(i,j,l)}/Q_{33})\mathcal{A}^2$, and $(\Delta_{(ij,kl)}/Q_{33})\mathcal{A}^2$ are either quadratic or cubic in $\mathcal{A}$. Dropping these terms yields $\mathcal{K}_{1,(i,j,l)} \approx 1$, $\mathcal{K}_{2,(i,j,l)} \approx (1 + \Delta_{(i,j,l)})/Q_{33} - 2\mathcal{A}$, $\mathcal{K}_{1,(ij,kl)} \approx 1$, and $\mathcal{K}_{2,(ij,kl)} \approx (1 + \Delta_{(ij,kl)})/Q_{33} - 2\mathcal{A}$.

Next, we denote $\mathcal{C}_{(i,j,l)} = c_{ii}n_1^2 + c_{jj}n_2^2 + c_{ll}n_3^2$ and $\mathcal{C}_{(ij,kl)} = (c_{ij} + c_{kl})n_in_j$ and simplify equation A-1 for weak attenuation and weak attenuation anisotropy as

$$\left[\mathcal{C}_{(1,6,5)}-\rho V^2+i\mathcal{C}_{(1,6,5)}\left(\frac{1+\Delta_{(1,6,5)}}{Q_{33}}-2\mathcal{A}\right)\right]$$
$$\times\left\{\left[\mathcal{C}_{(6,2,4)}-\rho V^2+i\mathcal{C}_{(6,2,4)}\left(\frac{1+\Delta_{(6,2,4)}}{Q_{33}}-2\mathcal{A}\right)\right]\right.$$
$$\times\left[\mathcal{C}_{(5,4,3)}-\rho V^2+i\mathcal{C}_{(5,4,3)}\left(\frac{1+\Delta_{(5,4,3)}}{Q_{33}}-2\mathcal{A}\right)\right]$$
$$\left.-\mathcal{C}^2_{(23,44)}\left[1+i\left(\frac{1+\Delta_{(23,44)}}{Q_{33}}-2\mathcal{A}\right)\right]^2\right\}$$
$$-\mathcal{C}_{(12,66)}\left[1+\left(\frac{1+\Delta_{(12,66)}}{Q_{33}}-2\mathcal{A}\right)\right]$$
$$\times\left\{\mathcal{C}_{(12,66)}\left[1+\left(\frac{1+\Delta_{(12,66)}}{Q_{33}}-2\mathcal{A}\right)\right]\right.$$
$$\times\left[\mathcal{C}_{(5,4,3)}-\rho V^2+i\mathcal{C}_{(5,4,3)}\left(\frac{1+\Delta_{(5,4,3)}}{Q_{33}}-2\mathcal{A}\right)\right]$$
$$-\mathcal{C}_{(13,55)}\left[1+\left(\frac{1+\Delta_{(13,55)}}{Q_{33}}-2\mathcal{A}\right)\right]$$
$$\left.\times\mathcal{C}_{(23,44)}\left[1+i\left(\frac{1+\Delta_{(23,44)}}{Q_{33}}-2\mathcal{A}\right)\right]\right\}$$
$$+\mathcal{C}_{(13,55)}\left[1+i\left(\frac{1+\Delta_{(13,55)}}{Q_{33}}-2\mathcal{A}\right)\right]$$
$$\times\left\{\mathcal{C}_{(12,66)}\left[1+i\left(\frac{1+\Delta_{(12,66)}}{Q_{33}}-2\mathcal{A}\right)\right]\right.$$
$$\times\mathcal{C}_{(23,44)}\left[1+i\left(\frac{1+\Delta_{(23,44)}}{Q_{33}}-2\mathcal{A}\right)\right]$$
$$-\mathcal{C}_{(13,55)}\left[1+i\left(\frac{1+\Delta_{(13,55)}}{Q_{33}}-2\mathcal{A}\right)\right]$$
$$\left.\times\left[\mathcal{C}_{(6,2,4)}-\rho V^2+i\mathcal{C}_{(6,2,4)}\left(\frac{1+\Delta_{(6,2,4)}}{Q_{33}}-2\mathcal{A}\right)\right]\right\}$$
$$=0. \tag{A-2}$$

The real part of equation A-2 is

$$(c_{11}n_1^2+c_{66}n_2^2+c_{55}n_3^2-\rho V^2)[(c_{66}n_1^2+c_{22}n_2^2+c_{44}n_3^2-\rho V^2)(c_{55}n_1^2+c_{44}n_2^2+c_{33}n_3^2-\rho V^2)-(c_{23}+c_{44})^2\,n_2^2n_3^2]-(c_{12}+c_{66})n_1n_2[(c_{12}+c_{66})\times n_1n_2(c_{55}n_1^2+c_{44}n_2^2+c_{33}n_3^2-\rho V^2)-(c_{13}+c_{55})(c_{23}+c_{44})n_1n_2n_3^2]+(c_{13}+c_{55})n_1n_3[(c_{12}+c_{66})(c_{23}+c_{44})n_1n_2n_3^2-(c_{13}+c_{55})n_1n_3(c_{66}n_1^2+c_{22}n_2^2+c_{44}n_3^2-\rho V^2)]=0, \tag{A-3}$$

which is identical to the Christoffel equation for the reference nonattenuative medium.

The normalized attenuation coefficient $\mathcal{A}$ is obtained from the imaginary part of equation A-2:

$$\mathcal{A}=\frac{1}{2Q_{33}}\left(1+\frac{\mathcal{H}_u}{\mathcal{H}_d}\right), \tag{A-4}$$

where

$$\mathcal{H}_u=\Delta_{(1,6,5)}\mathcal{C}_{(1,6,5)}[(\mathcal{C}_{(6,2,4)}-\rho V^2)\times(\mathcal{C}_{(5,4,3)}-\rho V^2)-\mathcal{C}^2_{(23,44)}]+\Delta_{(6,2,4)}\,\mathcal{C}_{(6,2,4)}\times[(\mathcal{C}_{(1,6,5)}-\rho V^2)(\mathcal{C}_{(5,4,3)}-\rho V^2)-\mathcal{C}^2_{(13,55)}]+\Delta_{(5,4,3)}\,\mathcal{C}_{(5,4,3)}[(\mathcal{C}_{(1,6,5)}-\rho V^2)(\mathcal{C}_{(6,2,4)}-\rho V^2)-\mathcal{C}^2_{(12,66)}]-2\Delta_{(13,55)}\,\mathcal{C}^2_{(13,55)}(\mathcal{C}_{(6,2,4)}-\rho V^2)-2\Delta_{(12,66)}\,\mathcal{C}^2_{(12,66)}(\mathcal{C}_{(5,4,3)}-\rho V^2)-2\Delta_{(23,44)}\,\mathcal{C}^2_{(23,44)}(\mathcal{C}_{(1,6,5)}-\rho V^2)+2(\Delta_{(13,55)}+\Delta_{(12,66)}+\Delta_{(23,44)})\,\mathcal{C}_{(13,55)}\,\mathcal{C}_{(12,66)}\,\mathcal{C}_{(23,44)} \tag{A-5}$$

and

$$\mathcal{H}_d=\rho V^2\,[(\mathcal{C}_{(1,6,5)}-\rho V^2)(\mathcal{C}_{(6,2,4)}-\rho V^2)+(\mathcal{C}_{(1,6,5)}-\rho V^2)\times(\mathcal{C}_{(5,4,3)}-\rho V^2)+(\mathcal{C}_{(6,2,4)}-\rho V^2)(\mathcal{C}_{(5,4,3)}-\rho V^2)-\mathcal{C}^2_{(12,66)}-\mathcal{C}^2_{(13,55)}-\mathcal{C}^2_{(23,44)}]. \tag{A-6}$$

The term $\mathcal{H}_u/\mathcal{H}_d$ in equation A-4 can be expressed through the velocity- and attenuation-anisotropy parameters. Assuming that the anisotropy is weak for both velocity and attenuation, we drop the quadratic and higher-order terms in all anisotropy parameters to obtain

$$\mathcal{H}_u=c_{33}(c_{33}-c_{55})^2\,[\epsilon_Q^{(2)}n_1^4+\epsilon_Q^{(1)}n_2^4+(2\epsilon_Q^{(2)}+\delta_Q^{(3)})n_1^2\,n_2^2+\delta_Q^{(2)}n_1^2n_3^2+\delta_Q^{(1)}n_2^2n_3^2],$$
$$\mathcal{H}_d=c_{33}(c_{33}-c_{55})\{(c_{33}-c_{55})(1+2\epsilon^{(2)}n_1^4+2\epsilon^{(1)}n_2^4+2\delta^{(2)}n_1^2n_3^2+2\delta^{(1)}n_2^2n_3^2+4\epsilon^{(2)}n_1^2n_2^2+2\delta^{(3)}n_1^2n_2^2)+c_{33}[\epsilon^{(1)}(-2n_2^2+6n_2^4)+\epsilon^{(2)}(-2n_1^2+6n_1^4+12n_1^2n_2^2)+6\delta^{(1)}n_2^2n_3^2+6\delta^{(2)}n_1^2n_3^2+6\delta^{(3)}n_1^2n_2^2]+2c_{55}[\gamma^{(1)}(-1-n_2^2)+\gamma^{(2)}(1-n_1^2)]\}. \tag{A-7}$$

Note that since $\mathcal{H}_u$ is linear in the anisotropy parameters, it is sufficient to keep just the isotropic part of $\mathcal{H}_d$. Substitution of equations A-6 and A-7 into equation A-4 yields the final form of the approximate P-wave attenuation coefficient given in the main text in equation 22.

REFERENCES

Akbar, N., J. Dvorkin, and A. Nur, 1993, Relating P-wave attenuation to permeability: Geophysics, **58**, 20–29.

Bakulin, A., V. Grechka, and I. Tsvankin, 2000, Estimation of fracture parameters from reflection seismic data-Part II: Fractured models with orthorhombic symmetry: Geophysics, **65**, 1803–1817.

Bakulin, A., and L. A. Molotkov, 1998, Application of complex Biot densities for the description of attenuation and dispersion in porous rocks: 60th Annual Conference and Exhibition, EAGE, Extended Abstracts, P085.

Brajanovski, M., B. Gurevich, and M. Schoenberg, 2005, A model for

P-wave attenuation and dispersion in a porous medium permeated by aligned fractures: Geophysical Journal International, **163**, 372–384.
Carcione, J. M., 1992, Anisotropic Q and velocity dispersion of finely layered media: Geophysical Prospecting, **40**, 761–783.
———, 2001, Wave fields in real media: Wave propagation in anisotropic, anelastic, and porous media: Pergamon Press, Inc.
Červený, V., and I. Pšenčík, 2005a, Plane waves in viscoelastic anisotropic media-I. Theory: Geophysical Journal International, **161**, 197–212.
———, 2005b, Plane waves in viscoelastic anisotropic media-II. Numerical examples: Geophysical Journal International, **161**, 213–228.
Crampin, S., 1981, A review of wave motion in anisotropic and cracked media: Wave Motion, **3**, 349–391.
———, 1991, Effects of singularities on shear-wave propagation in sedimentary basins: Geophysical Journal International, **107**, 531–543.
Grechka, V., A. Pech, and I. Tsvankin, 2005, Parameter estimation in orthorhombic media using multicomponent wide-azimuth reflection data: Geophysics, **70**, no. 2, D1–D8.
Grechka, V., S. Theophanis, and I. Tsvankin, 1999, Joint inversion of P- and PS-waves in orthorhombic media: Theory and a physical-modeling study: Geophysics, **64**, 146–161.
Grechka, V., and I. Tsvankin, 1999, 3-D moveout velocity analysis and parameter estimation for orthorhombic media: Geophysics, **64**, 820–837.
Helbig, K., 1994, Foundations of elastic anisotropy for exploration seismics: Pergamon Press, Inc.
Hosten, B., M. Deschamps, and B. R. Tittmann, 1987, Inhomogeneous wave generation and propagation in lossy anisotropic solids: Application to the characterization of viscoelastic composite materials: Journal of the Acoustical Society of America, **82**, 1763–1770.
Liu, E., S. Crampin, J. H. Queen, and W. D. Rizer, 1993, Velocity and attenuation anisotropy caused by microcracks and microfractures in a multiazimuth reverse VSP: Canadian Journal of Exploration Geophysics, **29**, 177–188.
Lynn, H. B., D. Campagna, K. M. Simon, and W. E. Beckham, 1999, Relationship of P-wave seismic attributes, azimuthal anisotropy, and commercial gas pay in 3-D P-wave multiazimuth data, Rulison Field, Piceance Basin, Colorado: Geophysics, **64**, 1293–1311.
MacBeth, C., 1999, Azimuthal variation in P-wave signatures due to fluid flow: Geophysics, **64**, 1181–1192.
Maultzsch, S., M. Chapman, E. Liu, and X.-Y. Li, 2003, Modeling frequency-dependent seismic anisotropy in fluid-saturated rock with aligned fractures: Implication of fracture size estimation from anisotropic measurements: Geophysical Prospecting, **51**, 381–392.
Mavko, G. M., and A. Nur, 1979, Wave attenuation in partially saturated rocks: Geophysics, **44**, 161–178.
Molotkov, L. A., and A. Bakulin, 1998, Attenuation in the effective model of finely layered porous Biot media: 60th Annual Conference and Exhibition, EAGE, Extended Abstracts, P156.
Parra, J. O., 1997, The transversely isotropic poroelastica newwave equation including the Biot and the squirt mechanisms: Theory and application: Geophysics, **62**, 309–318.
Pointer, T., E. Liu, and J. A. Hudson, 2000, Seismic wave propagation in cracked porous media: Geophysical Journal International, **142**, 199–231.
Prasad, M., and A. Nur, 2003, Velocity and attenuation anisotropy in reservoir rocks: 73rd Annual International Meeting, SEG, Expanded Abstracts, 1652–1655.
Schoenberg, M., and K. Helbig, 1997, Orthorhombic media: Modeling elastic wave behavior in a vertically fractured earth: Geophysics, **62**, 1954–1974.
Souriau, A., and B. Romanowicz, 1996, Anisotropy in inner core attenuation: A new type of data to constrain the nature of the solid core: Geophysical Research Letters, **23**, 1–4.
Stanchits, S. A., D. A. Lockner, and A. V. Ponomarev, 2003, Anisotropic changes in P-wave velocity and attenuation during deformation and fluid infiltration of granite: Bulletin of the Seismological Society of America, **93**, 1803–1822.
Stanley, D., and N. I. Christensen, 2001, Attenuation anisotropy in shale at elevated confining pressures: International Journal of Rock Mechanics & Mining Sciences, **38**, 1047- 1056.
Thomsen, L., 1986, Weak elastic anisotropy: Geophysics, **51**, 1954–1966.
Tsvankin, I., 1997, Anisotropic parameters and P-wave velocity for orthorhombic media: Geophysics, **62**, 1292–1309.
———, 2005, Seismic signatures and analysis of reflection data in anisotropic media, 2nd ed: Elsevier Science Publ. Co., Inc.
Willis, M., R. Rao, D. Burns, J. Byun, and L. Vetri, 2004, Spatial orientation and distribution of reservoir fractures from scattered seismic energy: 74th Annual International Meeting, SEG, Expanded Abstracts, 1535–1538.
Zhu, Y., and I. Tsvankin, 2006, Plane-wave propagation in attenuative transversely isotropic media: Geophysics, **71**, no. 2, T17–T30.
Zhu, Y., I. Tsvankin, P. Dewangan, and K. van Wijk, 2007, Physical modeling and analysis of P-wave attenuation anisotropy in transversely isotropic media: Geophysics, **72**, this issue.